

Generalizable Memory-driven Transformer for Multivariate Long Sequence Time-series Forecasting

Mingjie Li[†], Xiaoyun Zhao[†], Rui Liu, Changlin Li, Xiaohan Wang, and Xiaojun Chang

Abstract—Multivariate long sequence time-series forecasting (M-LSTF) is a practical but challenging problem. Unlike traditional timer-series forecasting tasks, M-LSTF tasks are more challenging from two aspects: 1) M-LSTF models need to learn time-series patterns both within and between multiple time features; 2) Under the rolling forecasting setting, the similarity between two consecutive training samples increases with the increasing prediction length, which makes models more prone to overfitting. In this paper, we propose a generalizable memory-driven Transformer to target M-LSTF problems. Specifically, we first propose a global-level memory component to drive the forecasting procedure by integrating multiple time-series features. In addition, we adopt a progressive fashion to train our model to increase its generalizability, in which we gradually introduce Bernoulli noises to training samples. Extensive experiments have been performed on five different datasets across multiple fields. Experimental results demonstrate that our approach can be seamlessly plugged into varying Transformer-based models to improve their performances up to roughly 30%. Particularly, this is the first work to specifically focus on the M-LSTF tasks to the best of our knowledge.

Index Terms—Multivariate Long Sequence Time-series Forecasting, Transformer, Memory-driven Forecasting, Generalizable Progressive Learning

I. INTRODUCTION

MULTIVARIATE long sequence time-series forecasting (M-LSTF) has solid practical implications for complex real-life scenarios. For example, hospital admission rates are dependent on factors such as time of day, season and current local influenza or COVID-19 trends, among others. The ability to predict hourly hospital admission rates days in advance can promote better shift allocation and medical supply management. With the success of deep neural networks (DNN) in many real-life scenarios [1]–[4], researchers start to investigate the effectiveness of DNNs in M-LSTF. Among all the DNNs, Transformer [5]-based models have demonstrated strong performance in long sequence time-series forecasting (LSTF) problems, for which they can predict hundreds of time steps ahead, in contrast to previous methods that were mostly only capable of making predictions for 48 time points or less [6], [7]. This is due to the fact that the Transformer’s self-attention mechanism allows models to learn interactions between data at different time points directly and works

well with large dimensional inputs and outputs [5]. However, existing LSTF Transformer models usually underperform in multivariate settings, in which models are asked to predict multiple target, simultaneously; because most existing LSTF methods primarily follow the objectives to reduce the computation costs for univariate predictions [8]–[10]. And thus, supervision signals and time sequential patterns from the rest variate are ignored.

There are two difficulties associated with applying Transformer models for M-LSTF problems leading to a lack of studies focusing on the specific characteristics of M-LSTF data. Firstly, the Transformer was originally designed for language analysis [5], [11], [12], which can be seen as a single series of sequential data; Layer Normalization [13] is adopted to reduce the training times similar to other recurrent neural networks; hence, its ability to analyze interactions between different data series is limited. Different from the natural language processing tasks, normalization operation should also be conducted within the same variant in one batch, since target and source sequences may be in separate order of magnitude. As a result, the Transformer architecture can be inadequate for multivariate problems. Secondly, LSTF is more prone to overfitting than short-term forecasting because it requires models to have larger dimensions to accommodate larger input and output sizes, which leads to increased training parameters. In addition, models are trained under a rolling forecasting setting as common practice for time-series forecasting (See Figure 1 for more details). However, under the rolling forecasting setting, if the stride size is 1, then the previous and current training samples are only one data point apart from each other. Since making longer predictions typically requires longer input sequences, training samples for LSTF models have a higher degree of similarity. For example, when the model’s input length is 2, the similarity between two consecutive training inputs is 50% (1/2); however, if we increase the model’s input length to 168, the similarity between two consecutive training inputs rises to 99.4% (167/168). Therefore, the LSTF models are more likely to suffer from overfitting due to high data similarity. One could argue that we could decrease the training sample similarities by increasing the stride size; however, the number of training samples decreases by the factor of the stride size, as the training sample numbers are calculated by:

$$N_t = \frac{N_d - S_w + 1}{S_s}. \quad (1)$$

Where N_t represents the number of training samples, N_d represents the total number of time points in the training

M. Li, C. Li and X. Chang are with The ReLER Lab, Australian Artificial Intelligence Institute, Faculty of Engineering and Information Technology, University of Technology Sydney, Australia (e-mail: mingjie.li, changlin.li@monash.edu, xiaojun.chang@uts.edu.au).

X. Zhao and R. Liu are with the Faculty of Information Technology, Monash University.

X. Wang is with College of Computer Science and Technology, Zhejiang University, China.

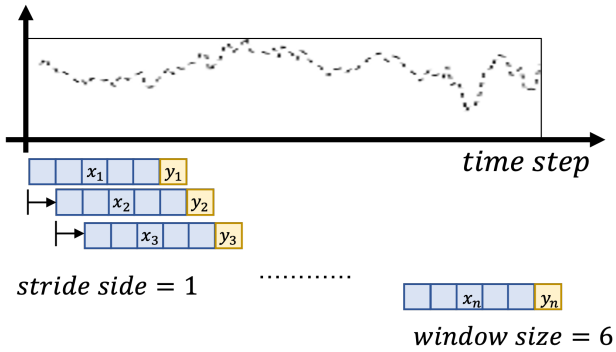


Fig. 1: The illustration of the rolling forecasting setting with stride size=1.

data, S_w refers to the window size, and S_s is the stride size. Although increasing stride sizes can decrease the sample similarities, it causes a decrease in training sample numbers, which also increase the likelihood of overfitting.

Our work specifically targets the aforementioned difficulties. To address the first problem, we focus on improving the Transformer’s ability to recognize more complicated sequential patterns from highly similar training data, thereby increasing a model’s ability to address M-LSTF problems. This is achieved by adopting a global-level memory-driven transformer approach, which both effectively utilizes the past time-series information and introduces further calculations to enhance the model’s ability on complex pattern recognition. Moreover, layer normalization is replaced by batch normalization in the backbone Transformer encoder layers to improve the communication within the same batch. To address the second limitation, we adopt a progressive training schedule to increase the model’s generalization power. Here, we leverage the concept of curriculum learning, whereby we gradually increase the training task difficulty and data variety by progressively introducing Bernoulli noises to the training data via a dynamic dropout scheme that can effectively reduce overfitting and increase the model performance. The main contributions of this paper are summarized as follows:

- We propose to forecast multivariate long sequence time-series data via a generalizable memory-driven transformer. This is the first work focusing on multivariate long sequence time-series forecasting to the best of our knowledge.
- We propose a global-level memory matrix to drive the forecasting process and employ a progressive training schedule to improve the generalizability of our method.
- Extensive experiments are performed, and the results show that our method can be seamlessly plugged into different transformer-based models and improve their performances.

II. RELATED WORK

A. Time-Series Transformer Models

Time-series tasks [14]–[18] along with varying real-life scenarios have attracted increasing attentions from researchers in machine learning and deep learning fields. Recently,

Transformer-based models have achieved state-of-the-art results in many time-series tasks [8], [10], [19]–[22], especially in LSTF problems [8]–[10], [21]. There are several areas of focus among the latter studies. Some have focused on reducing the computational costs to enable longer predictions by sparse attention, whereby the memory cost is reduced from $O(L^2)$ to as low as $O(L \log L)$ [8]–[10], where L refers to the sequence length in attention layers. Studies have also changed the architecture to further enhance the Transformer’s ability to learn time-series patterns [21]. However, all of these studies primarily focus on univariate long sequence time-series forecasting (U-LSTF) problems. Since M-LSTF problems require the model to also understand time-series interactions across multiple features, M-LSTF should be treated differently than U-LSTF.

B. Memory-Driven Transformers

The concept of the memory component originated from [23] where it allows the model to better remember the past inputs in NLP. Since then, this concept has been further developed by multiple researchers [24]–[26]. In the recent two years, many researchers have been applying this idea on Transformer-based models across a variety of topics such as medical report generation [27], [28], question and answer modelling [29], video captioning [30], speech recognition [31], [32] and machine translation [33], [34] *etc.* These studies suggest that the memory block is effective in reinforcing the model to learn the complicated sequential patterns. Since time-series data also have a strong sequential pattern, the memory unit should further improve the existing Transformer methods on the time-series problems.

C. Progressive Training Strategy

In recent years, researchers have come up with various progressive training strategies to help models learn from complex datasets, in which the researchers design special training schedules to allow gradual improvements of models throughout their training processes. This concept has been widely used across multiple fields, such as computer vision [35]–[37] and NLP [38]. There are many different ways of practising progressive training. An example of such practice is progressive curriculum learning (CL) defined by [39], in which it is a newer type of CL that is not directly related to sample difficulty [40], but rather entails a progressive adaption of the task setting. [41] utilized this approach in developing a “curriculum dropout” function that provides a time schedule to monotonically increase the number of model parameters expected to be suppressed based on a Bernoulli distribution; they suggest that the dropout rate should be lower at the start and progressively increase throughout the training process. Since there is a proven connection between the dropout and data noises [42]–[44], by applying such a function, we can introduce further noises to the data, which indirectly increases the prediction tasks’ difficulties over training epochs. The authors have conducted extensive experiments over a range of datasets and showed that the approach can effectively address overfitting issues and increase model performance.

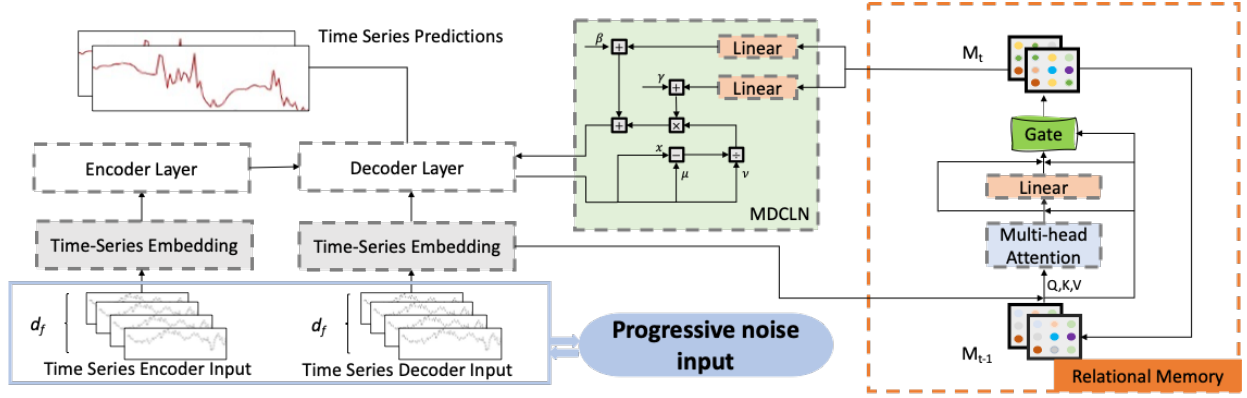


Fig. 2: An overview of the model architecture, where the structure of the memory-driven transformer is presented. M_{t-1} represents the memory matrix from the previous prediction, M_t represents the updated memory matrix during the current sequence prediction, which in turn is recycled to be the M_{t-1} for the next prediction.

III. APPROACH

In this section, we present our method that specifically targets the challenges for M-LSTF. Our approach is based upon the Transformer architecture; we aim to enhance Transformer models on M-LSTF problems by making improvements from both the architectural and training optimization prospects. The overview of our approach is illustrated in Figure 2. Our model comprises three major elements, namely the input embedding, the main Transformer-based model and the memory component, whereby we propose to train the model based on a progressive strategy. A description of the first two units is presented in the § III-B, and the memory component is described in the remaining subsections.

A. Problem Setup

Typical time-series models normally train under rolling forecasting settings with a fixed window and a stride size = 1, as shown in Figure 1. The input data at time t can be written as $X^t = \{x_1^t, x_2^t, \dots, x_{L_S}^t | x_k^t \in R^{d_f}\}$, where L_S is the input length and the feature dimension $d_f > 1$. Moreover, the model output is $Y^t = \{y_1^t, y_2^t, \dots, y_{L_p}^t\}$, where L_p is the prediction length, and the output feature dimension is flexible and is not limited to single sequence predictions.

B. Base Model

1) *Input Embedding*: The input data are first passed through an embedding. Different from other types of sequential data, in time series problems, the model should capture the time information. This is extremely crucial in LSTF settings, as models are required to make predictions up to weeks in advance. We decided to utilize the time-series specific embedding method proposed by [10]. The method applies a combination of the context vector, the positional embedding and the seasonal embedding. The context vector $u^t \in R^{L_S * d_{model}}$ is obtained by projecting the model input $X^t \in R^{L_S * d_f}$ into a dimension of d_{model} by an 1-D convolutional layer. The goal of the context vector is to transform the input data into an appropriate dimension. The positional embedding (PE(pos)) and the seasonal embedding (SE(pos)) are used to capture the local context and

the global time feature, respectively. The formula for the input embedding is:

$$X_{embed}^t = \delta u^t + \text{PE}(\text{pos}) + \sum_k [\text{SE}(\text{pos})]_k \quad (2)$$

Where $X_{embed}^t \in R^{L_S * d_{model}}$ is the embedded model input, δ is the weight factor to balance between the embeddings and the context vector and k represents the levels of the seasonal components, *i.e.* days, weeks, seasons, holidays.

2) *Encoder-Decoder Architecture*: The backbone of our method lies on Transformer-based models following an encoder-decoder structure. Notably, we replace the layer normalization by batch normalization in Transformer encoder layers to improve the communication between different sequences within one batch. Despite some minor differences between different variants, their general purpose is the same. The encoder takes past input sequences into the model and generates hidden states as outputs that contain time pattern information, which the decoder uses to make predictions. We decided to use generative-style decoding, which has been proven to achieve superior performances in LSTF problems and have exponentially better computational efficiency than conventional dynamic decoding [11]. The generative-style decoding generates all predictions in one step, with the decoder feeding vector $X_{feed,dec}^t$ presented as:

$$X_{feed,dec}^t = \text{Concat}(X_{dec}^t, X_0^t) \in R^{(L_{dec} + L_p) * d_f} \quad (3)$$

where $X_{dec}^t \in R^{L_{dec} * d_f}$ is the time-series input sequence for the decoder, L_{dec} is the length of the decoder time-series input, $X_0^t \in R^{L_p * d_f}$ is the placeholder for the prediction sequence, and the L_p is the prediction length.

C. Memory-driven Forecasting

Applications of the memory concept have demonstrated superior performances in a variety of sequential tasks [45]–[47]. In particular, [48] demonstrated that the memory concept is effective in improving LSTM’s ability on multivariate time-series forecasting. Therefore, this concept should also work

on Transformer models under the multivariate forecasting setting. There are various ways of implementing memory into Transformers [27], [29], [49]–[53]. Our goal is to enhance the Transformer’s ability on both handling increased data complexity brought by multivariate data and recognizing hidden sequential patterns from highly similar training data. We decide to incorporate a memory unit into the decoder block because the decoder block is highly relevant to the output predictions. Our work is based on the relational memory proposed by [27], as it has proven successful in the case of medical report generation, in which reports are all highly similar and follow a strict structure. The relational memory has a self-attention layer which can help to further analyze the hidden sequential patterns that are missed by the encoder-decoder component through combining information stored in the memory matrix together with the model input. To further improve this concept, we make the relational memory unit function at a global level to suit the time-series features. The way to connect the relational memory block to the decoder is via a memory-driven conditional layer normalization (MDCLN) layer, the general formula for this connection can be written as:

$$\text{MDCLN}(\text{Att}(h_{l-1}), M_t) \quad (4)$$

where $\text{MDCLN}(\cdot)$ is the memory-driven conditional layer normalization, $\text{Att}(\cdot)$ represents the attention layer in the decoder block, h represents the output state from the previous layer $l - 1$, and M_t refers to the updated memory matrix at time point t .

1) *Memory-driven Conditional Layer Normalization*: The Memory-driven Conditional Layer Normalization (MDCLN) is a way to integrate relational memory into the decoder [27] (See Figure 2 for the architecture overview), where outputs from the decoder’s self-attention layer undergoes layer normalization along with the memory information provided from the relational memory block. The reason for using layer normalization instead of batch normalization is that input data are normalized before feeding into models as common practice for time-series forecasting. Hence, instead of normalizing values among batches, we use layer normalization to normalize the features within each batch to give each time feature an equal weight for generating predictions.

In MDCLN, we update γ and β based on the memory matrix M_t , as they are the two most essential parameters for normalization:

$$\gamma_t = \gamma + f_l(M_t), \quad (5)$$

$$\beta_t = \beta + f_l(M_t). \quad (6)$$

Where $f_l(\cdot)$ represents the linear layer. The MDCLN is achieved by:

$$\text{MDCLN}(h_{l-1}, M_t) = \gamma_t \odot \frac{h_{l-1} - \mu}{\sigma} + \beta_t + f_l. \quad (7)$$

Where μ and σ are the mean and standard deviation of h_{l-1} , and h_{l-1} is the output of self-attention at layer $l - 1$ in the decoder.

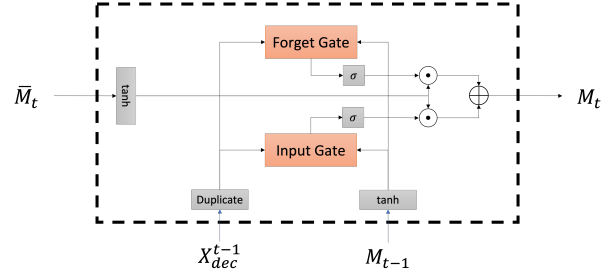


Fig. 3: Overview of the gate mechanism.

2) *Global-level Memory Matrix*: In addition to the further calculations that the relational memory unit can bring, another main characteristic of this unit is that it can read/write information from/to a memory matrix which assists with analyzing time patterns. In NLP problems, researchers use dynamic decoding [11]; the memory matrix works by maintaining information from the prediction of the last token/word while predicting a paragraph, and this matrix is re-initialized after each paragraph, as each paragraph is perceived as being independent [27]. However, as explained above, we use generative-style decoding for our task, in which it generates all predictions in a single step [10]. In this case, the traditional matrix initialization method will not work, as we do not generate individual time point predictions one by one. In addition, for each forecasting problem, the input sequences for making previous predictions are still helpful for any future prediction, as they come from the same time series and share similar pattern interactions. Therefore, we adjust the matrix initialization method to a global level. We maintain a memory matrix for each specific forecasting task, where we keep the matrix output from the relational memory at the prediction time point $t - 1$ as the input matrix at time point t ; this matrix is updated after every prediction by a gating mechanism to control the ratio of the memory matrix being updated. Since more recent model inputs are weighted higher than those from the distant past, the matrix can maintain all relevant time information. In addition, this matrix will continue updating even after training, which ultimately increases the model’s generalization power. The relational memory unit updates the memory matrix by first calculating the self-attention based on the matrix M at time point $t - 1$, where $Q = M_{t-1} \times W_q$, $K = [M_{t-1}; \text{embed}(X_{\text{feed,dec}}^t)] \times W_k$ and $V = [M_{t-1}; \text{embed}(X_{\text{feed,dec}}^t)] \times W_v$. The W_k , W_v and W_q are trainable weights, and $[M_{t-1}; \text{embed}(X_{\text{feed,dec}}^t)]$ is the row-wise concatenations between M_{t-1} and the embedded decoder feeding vector. We then calculate the self-attention score Z from Q , K and V . After the self-attention layer, we go through a feed-forward layer to produce \bar{M}_t , which is calculated as:

$$\bar{M}_t = \text{Feedforward}(Z + M_{t-1}) + Z + M_{t-1} \quad (8)$$

\bar{M}_t is then passed through a gating mechanism to calculate the ratio of the \bar{M}_t to be added to the final M_t :

$$M_t = \sigma(G_f^t) \odot M_{t-1} + \sigma(G_i^t) \odot \bar{M}_t \quad (9)$$

where G_i^t is the input gate, G_f^t is the forget gate, \odot is the Schur product, and $\sigma(\cdot)$ is the Sigmoid function.

TABLE I: The comparison of our method with the Transformer baselines, where ProbTrans is the Transformer with ProbSparse attention (three repetitions). The numbers in bold represent the better-performed models in each Transformer-based model pair.

method		Informer+ours		Informer		Transformer+ours		Transformer		ProbTrans+ours		ProbTrans	
metric		MSE	MAE	MSE	MAE	MSE	MAE	MSE	MAE	MSE	MAE	MSE	MAE
Etth1	24	0.495	0.493	0.550	0.541	0.474	0.493	0.456	0.474	0.514	0.513	0.453	0.476
	48	0.582	0.555	0.644	0.606	0.585	0.568	0.608	0.584	0.579	0.540	0.649	0.607
	168	0.981	0.771	1.110	0.861	0.914	0.750	0.925	0.767	0.941	0.753	1.160	0.876
	336	1.098	0.816	1.237	0.893	1.001	0.801	1.077	0.821	1.122	0.847	1.461	0.982
	720	1.156	0.842	1.475	0.993	1.164	0.871	1.182	0.872	1.336	0.931	1.550	1.032
Etth2	24	0.542	0.560	0.385	0.467	0.534	0.581	0.474	0.522	0.759	0.701	0.416	0.485
	48	1.190	0.873	1.959	1.119	0.909	0.761	1.063	0.832	1.136	0.850	1.598	1.006
	168	4.869	1.856	5.957	2.036	4.951	1.807	4.067	1.623	5.560	2.000	6.166	2.191
	336	4.672	1.872	4.303	1.780	4.371	1.727	3.852	1.613	4.982	1.932	4.650	1.881
	720	3.358	1.569	3.444	1.574	3.690	1.671	2.603	1.369	3.347	1.591	2.791	1.429
Air	24	0.542	0.374	0.562	0.388	0.560	0.383	0.552	0.380	0.559	0.388	0.552	0.380
	48	0.650	0.435	0.692	0.447	0.679	0.440	0.698	0.448	0.653	0.443	0.673	0.441
	168	0.720	0.479	0.883	0.518	0.780	0.502	0.798	0.499	0.770	0.498	0.770	0.503
	336	0.773	0.505	0.852	0.536	0.789	0.501	0.823	0.514	0.764	0.496	0.831	0.527
	720	0.793	0.503	0.861	0.534	0.840	0.514	0.859	0.524	0.831	0.516	0.870	0.541
Traffic	24	0.324	0.222	0.381	0.264	0.337	0.248	0.411	0.282	0.345	0.247	0.414	0.283
	48	0.351	0.243	0.440	0.300	0.364	0.275	0.486	0.336	0.360	0.262	0.480	0.333
	168	0.405	0.300	0.567	0.396	0.407	0.300	0.555	0.384	0.439	0.323	0.547	0.380
	336	0.397	0.291	0.572	0.399	0.413	0.302	0.570	0.400	0.446	0.324	0.572	0.398
	720	0.468	0.330	0.585	0.400	0.392	0.293	0.585	0.399	0.482	0.339	0.590	0.403
Weather	24	0.253	0.338	0.258	0.342	0.253	0.340	0.263	0.352	0.253	0.341	0.266	0.348
	48	0.344	0.411	0.354	0.418	0.338	0.414	0.348	0.419	0.371	0.443	0.367	0.429
	168	0.507	0.520	0.578	0.544	0.513	0.512	0.551	0.526	0.517	0.515	0.578	0.557
	336	0.545	0.537	0.591	0.553	0.512	0.507	0.584	0.547	0.560	0.545	0.630	0.579
	720	0.593	0.648	0.625	0.567	0.554	0.530	0.642	0.576	0.620	0.566	0.651	0.588

3) *Gate Mechanism*: The gate mechanism decides the proportion of new information from \bar{M}_t to incorporate and the proportion of M_{t-1} to discard to produce the final M_t . The gate mechanism has two key components: the input gate G_i^t and the forget gate G_f^t . The two gates are calculated by balancing the embedded decoder input $X_{feed,dec}^{t-1}$ and the previous memory matrix at $t-1$ (M_{t-1}), where we duplicate the $embed(X_{feed,dec}^{t-1})$ to match the dimension of M_{t-1} (See Figure 3). These two gates have the formulas:

$$G_i^t = embed(X_{feed,dec}^{t-1}) \times W_i + \tanh(M_{t-1}) \times U_i, \quad (10)$$

$$G_f^t = embed(X_{feed,dec}^{t-1}) \times W_f + \tanh(M_{t-1}) \times U_f. \quad (11)$$

Where W_i , W_f , U_i , and U_f are trainable weights for the two gates.

D. Generalizable Progressive Training

Overfitting is one of the main drawbacks of M-LSTF models due to the increased model dimension and a high degree of the training sample similarity. The increased model dimension is unavoidable, as the model input and output must increase when predicting long sequence predictions. Therefore, we decided to mitigate the problem from the training sample perspective under the rolling forecasting setting. However, as mentioned in the introduction, increasing stride size for the rolling window does not help with the overfitting issue. We decided to target the overfitting issue by adding sample variety. These noises should be added in a manner such that the rate is slower at the beginning to ensure that the model has a good grasp

of the data pattern before we start to increase the rate of introducing noises to prevent the model from overfitting. To achieve this goal, we decided to alter dropout rates, as there is a proven connection between dropout and noises [42]–[44]. We dynamically alter the dropout rate during training based on a monotone function proposed by [41], whereby the function rate starts slower and later increases as training proceeds. The dropout rate function is based on:

$$\theta_d(t) = \min(\theta_{max}, 1 - \theta_{max} - (1 - \theta_{max}) \exp(-\gamma t)) \quad (12)$$

where t is the t^{th} number of 100 iterations, θ_d is the dropout rate, θ_{max} is the maximum dropout rate, and γ is a hyper-parameter typically set between 0.001 to 0.01.

1) *Loss function*: The loss function we use is Mean Squared Error (MSE) loss on the target sequences, and it is then back propagated across the entire network.

$$L_{MSE} = \frac{1}{n} \sum_{i=1}^n (y_i - \hat{y}_i)^2, \quad (13)$$

where y_i is the true value for the i^{th} time step in the output sequence, \hat{y}_i is the predicted value, and n is the total number of values. Both y_i and \hat{y}_i have a dimension of ≥ 1 .

IV. EXPERIMENTS

A. Datasets

We conduct extensive experiments on 5 public benchmark datasets from 4 sources.

ETT (Electricity Transformer Temperature) [10]. The dataset contains information about six power load features and the

target value ‘‘oil temperature’’. We use the two hourly datasets from the source named as $Etth_1$ and $Etth_2$. We use the first 20 months of data and the train/val/test splits follow the ratio of 6/2/2.

Weather (Local Climatological Data)¹. The dataset contains hourly data about climate information from around 1,600 locations in USA between 2018 and 2020. The data consist of seven quantitative climatological features with ‘‘dry bulb temperature’’ as the target. The train/val/test ratio is 7/1/2.

Air Quality (Beijing Multi-site Air-Quality Data)². The dataset consists of eleven quantitative hourly features relevant to air quality with the target value set as ‘‘PM10’’ from 12 national air quality monitoring sites. We use the data from the ‘‘Wanshouxigong’’ station. The train/val/test follows the ratio of 7/1/2.

Traffic (Metro Interstate Traffic Volume)³. The dataset contains the traffic condition data measured in the of between Minneapolis and St Paul, Minnesota, USA. The datasets has five hourly numerical features with the target value of ‘‘traffic volume’’. The train/val/test ratio is 7/1/2.

B. Experimental Details

1) *Baselines*: We use three Transformer variants as our baseline with generative-style decoding to generate the output sequences in one step [10]. The three Transformer-based models are the Transformer model with canonical attention [5], the Transformer model with ProbSparse attention [10] and the Informer model [10]. In addition, we compared our model’s performance with two classical DNN time-series methods: the LSTM [54] and LSTnet [55].

2) *Implementation Details*: Our model is constructed based on Pytorch with Python 3.7. We use a single NVIDIA Tesla V100 GPU for training. All of the input data undergo normalization before being fed into the model. The training is performed under the rolling forecasting setting (stride size=1). The encoder and decoder input lengths are {48,96,168,168,336} and {48,48,168,168,336}, which correspond to the prediction lengths of {24,48,168,336,720}, respectively. For the progressive training scheme, we update the dropout rate for every 100 iterations with the upper dropout limit of 0.1. More details of the model parameters are presented in the Appendix C. Moreover, we apply early stopping technique with patience=3 during training and the training epoch is set to be 6. The learning rate starts from 0.0001 and it halves its value for every epoch after the first two epochs.

3) *Evaluation Metrics*: We use two evaluation metrics to measure our model performance: Mean Squared Error (MSE) and Mean Absolute Error (MAE).

4) *Model Reproducibility*: To ensure the model reproducibility, we present detailed parameter settings in this section. Table II describes the details for all Transformer-based models. We use the same setting for all three Transformer-based models in our experiment because these three models

¹<https://www.ncei.noaa.gov/data/local-climatological-data>

²<https://archive.ics.uci.edu/ml/datasets/Beijing+Multi-Site+Air-Quality+Data>

³<https://archive.ics.uci.edu/ml/datasets/Metro+Interstate+Traffic+Volume>

TABLE II: Key parameters for transformer-based models.

Prediction Len.	{24,48}	{168,336}	{720}
d_{model}	1024	1024	1024
d_{ff}	2048	2048	2048
n_heads	8	8	8
Dropout	0.1	0.1	0.1
Activation	GELU	GELU	GELU
Batch Size	32	8	4
Enc.Layer no.	1	2	2
Dec.Layer no.	1	1	1

TABLE III: Key parameters for the relational memory unit.

	Informer	Transformer	ProbTrans
d_{rm}	1024	1024	1024
Mem.slot.no.	1	2	2
Mem.head.no.	4	2	2

share a very similar structure and show optimal performance under similar settings. However, we use different settings for different prediction output lengths to adjust the model for different prediction tasks. Table II specifies the model dimension (d_{model}), the dimension of positional feed-forward layers inside the encoder and decoder block (d_{ff}), and the number of attention heads in each attention layer (n_heads). In addition, we include information about batch size, layer activation function, the encoder layer number (Enc.Layer no.), and the decoder layer number (Dec.Layer no.). Table III describes the parameters for the relational memory block. There are three key parameters for the relational memory unit: the unit dimension (d_{rm}), the number of memory units (Mem.slot.no), and the number of attention heads in the relational memory (Mem.head.no). Here, we apply different relational memory settings for the three Transformer-based models as they require different settings to achieve optimal performance.

C. Results and Analysis

1) *Comparison with baselines*: Table I summarizes the results of the Transformer baselines and our proposed methods. We applied the same setting for each transformer-based model pair to achieve a fair comparison. Based on the results in Table I, we find that: (1) Our model can significantly improve the Transformer-based model’s performance up to 30% on M-LSTF problems across most cases; it improves the MSE

TABLE IV: Comparison of our method with other DNN methods on Multivariate Long Sequence Time. The results of the DNN methods sourced from [10].

Methods	Informer+ours		LSTM		LSTnet		
	MSE	MAE	MSE	MAE	MSE	MAE	
Etth1	24	0.495	0.493	0.650	0.624	1.293	0.901
	48	0.582	0.555	0.702	0.675	1.456	0.960
	168	0.981	0.771	1.212	0.867	1.997	1.214
	336	1.098	0.816	1.424	0.994	2.655	1.369
	720	1.156	0.842	1.960	1.322	2.143	1.380
Etth2	24	0.542	0.560	1.143	0.813	2.742	1.457
	48	1.190	0.873	1.671	1.221	3.567	1.687
	168	4.869	1.856	4.117	1.674	3.242	2.513
	336	4.672	1.872	3.434	1.549	2.544	2.581
	720	3.358	1.569	3.963	1.778	4.625	3.709

TABLE V: Ablation study for the decomposition of our approach, where p.t. is the progressive training scheme and mem refers to our memory approach (three repetitions).

datasets		Eth1				Air quality				Traffic			
prediction		24	48	168	336	24	48	168	336	24	48	168	336
Informer	MSE	0.550	0.644	1.110	1.237	0.562	0.692	0.833	0.852	0.381	0.440	0.567	0.572
	MAE	0.541	0.606	0.861	0.893	0.388	0.447	0.518	0.536	0.264	0.300	0.396	0.399
Informer + p.t.	MSE	0.510	0.651	1.021	1.136	0.583	0.690	0.813	0.848	0.377	0.431	0.564	0.571
	MAE	0.514	0.608	0.820	0.820	0.387	0.447	0.524	0.535	0.262	0.290	0.389	0.398
Informer + mem	MSE	0.510	0.588	1.009	1.161	0.569	0.680	0.769	0.794	0.331	0.352	0.411	0.417
	MAE	0.506	0.556	0.810	0.827	0.386	0.438	0.496	0.516	0.228	0.249	0.302	0.306
Informer + ours	MSE	0.495	0.582	0.981	1.098	0.542	0.650	0.720	0.773	0.324	0.351	0.405	0.397
	MAE	0.493	0.555	0.771	0.816	0.374	0.435	0.479	0.505	0.222	0.243	0.300	0.291

TABLE VI: Ablation study of different memory matrix initialization methods (three repetitions).

datasets		Eth1				Eth2				Weather			
prediction		24	48	336	720	24	48	168	336	24	48	168	336
Informer+mem (Ours)	MSE	0.510	0.588	1.009	1.161	0.553	1.204	5.069	4.883	0.243	0.350	0.519	0.556
	MAE	0.506	0.556	0.810	0.843	0.578	0.879	2.043	1.896	0.328	0.411	0.525	0.549
Informer+mem (Original)	MSE	0.537	0.571	1.168	1.224	0.592	1.242	6.454	5.034	0.254	0.353	0.521	0.567
	MAE	0.528	0.546	0.848	0.894	0.602	0.888	2.251	1.943	0.335	0.412	0.530	0.544

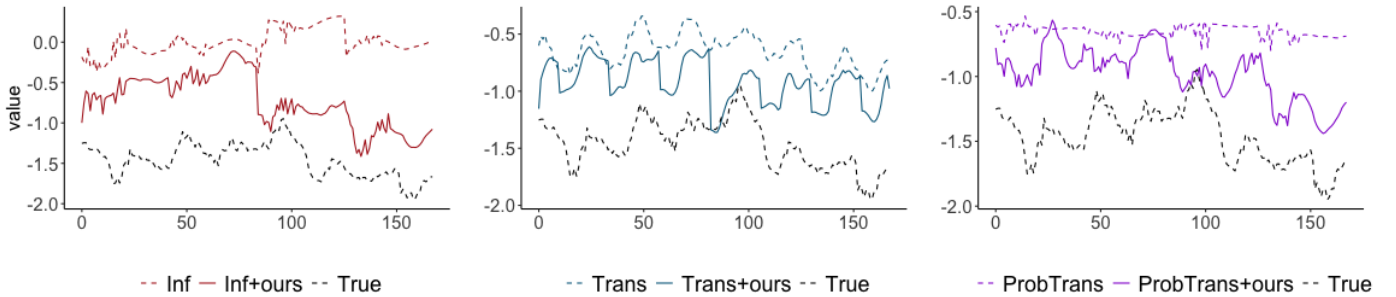


Fig. 4: The test results of applying our proposed memory unit to different Transformer-based models on the Eth1 dataset with the prediction length of 168.

and MAE scores in 23 of 25 prediction tasks in Informer, 20 of 25 tasks in Transformer with canonical attention, and 20 of 25 tasks in Transformer with Prob-Sparse attention. Our results show that our proposed memory-driven approach with the progressive training schedule can help Transformers with M-LSTF problems. (2) Our method works particularly well in longer prediction settings. For instance, when the prediction length is 720, our approach improves the Informer’s MSE score by 21.63% for the Eth1 dataset and 20.00% for the traffic dataset, in contrast to the 10.00% and 14.96% improvements, respectively, for the prediction length of 24, and this trend is consistently observed across all different models and datasets. The improved performance with longer prediction settings makes sense, considering that the relational memory unit is highly effective at dealing with highly similar data, and our progressive training strategy effectively addresses the overfitting issues caused by increased prediction lengths.

Apart from the Transformer baselines, in Table IV, we also compare our methods with the prediction results from two classical time-series deep neural network (DNN) methods, namely the LSTM and LSTnet, from [10]. We can see the Informer+ours method outperforms LSTM and LSTnet in all tasks in the Eth1 dataset and 3 of the 5 prediction tasks in the Eth2 dataset. When the prediction length is 720, the Informer+ours method achieves a 41.02% and 36.79%

improvement on the MSE and MAE scores over LSTM and a 46.05% and 38.98% improvement on the MSE and MAE scores over LSTnet for the Eth1 dataset. For the Eth2 dataset, we also observe a substantial improvement of up to 57.70% on the MSE and MAE scores when using our proposed approach. Although LSTM and LSTnet perform better with the Eth2 dataset than our approach, this could be due to the differences caused by the datasets, which is extremely common in time-series forecasting [10], [56]. Such variations could be explained by the “no free lunch theorem” [57], as different time-series data can have completely distinct patterns, it is extremely difficult to create a model that fits all kinds of data. Overall, our approach demonstrates remarkable improvements over the classical DNN methods in most settings.

2) *Case Study*: Figure 4 is a visualization of time series predictions by different models on the Eth1 dataset (More examples are presented in the Appendix D). Based on these plots, we can observe that the proposed memory unit can better maintain short-term fluctuations or the seasonal component of data. In particular, in the case of the Transformer with Prob-Sparse attention, we can see that the memory unit helps the model to capture the seasonal component very well, such that the short-term fluctuations are better captured by the model with the proposed memory unit, in contrast to the predictions for the model without the memory unit, for which the trend

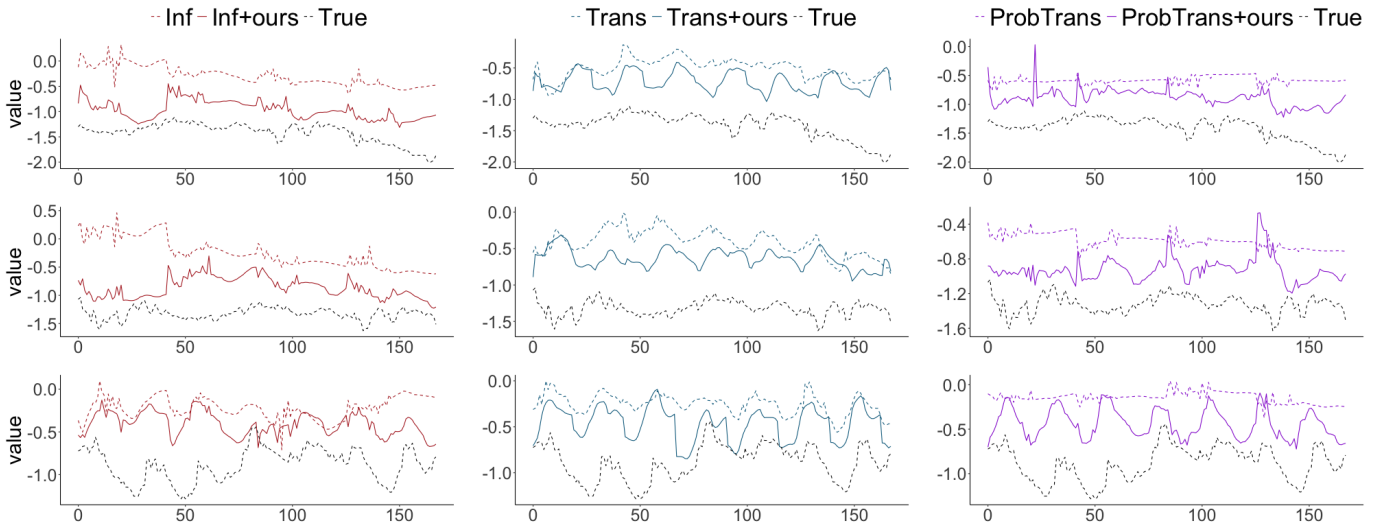


Fig. 5: The test results of applying our methods on different Transformer-based models on the Etth1 dataset with the prediction length of 168.

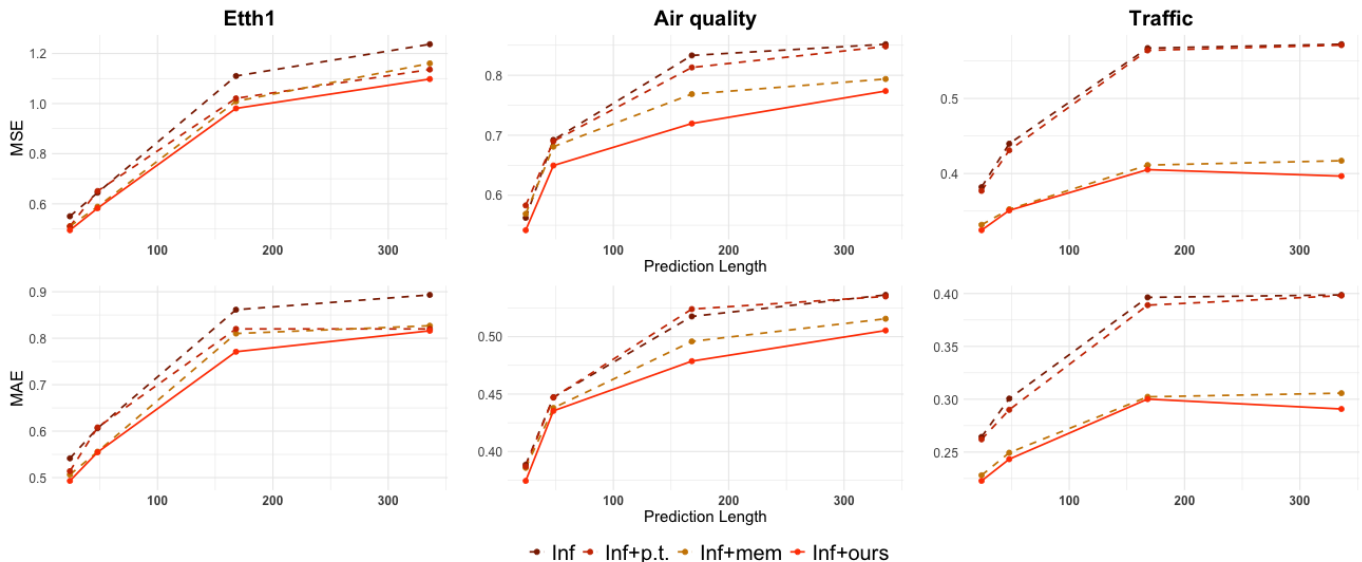


Fig. 6: Visualizing the effects of our approach by testing each individual component on the Etth1 dataset, where p.t. refers to our proposed progressive training schedule, and mem refers to our proposed memory approach (the relational memory unit).

line stays relatively smooth and does not vary much across time. This result demonstrates that our relational memory block is able to detect patterns from highly similar data and is very sensitive to small data changes, which enhances the model’s ability to learn from the seasonal component of the time-series data.

Figure 5 shows the performance differences between the Transformer-based models and our method, where each row represents a different test sample, and each column represents a different Transformer-based model class. These test samples are different from the one presented in the main article section; they serve as an additional demonstration of our proposed model’s performance. Based on Figure 5, most of our proposed approach’s predictions are closer to the true values than their base model’s predictions, reflecting our

proposed approach’s superiority. In addition, we can see that our approach is better at capturing the short-term fluctuations than the Transformer-based models, as the prediction trend lines for the Transformer-based models are smoother and does not vary much across time, which demonstrates that our model can detect more minor data changes.

3) *Visualization of the performance of our approach:* The line plots present in Figure 6 visualize the performance of each of our approach’s components and their combined effects on the Informer, based on the Etth1 dataset. The figure serves to complement the first ablation study in the main article. The purpose of including these plots is to demonstrate the effects of our approach visually. We can see that both the memory and the progressive training strategy can increase the Transformer-based model’s performances individually on

both MSE and MAE. However, their combined effects are more prominent than their individual effects indicating that our proposed approach utilizes an effective combination of these two components. It is also worth noting that the effectiveness of our method increases as the prediction length increases.

4) *Ablation Study*: We performed two ablation studies to better understand the performance of our model. We first ran experiments on the Eth1, Air Quality and Traffic dataset and compared the performance of the different components of our proposed methods. We summarize the results in Table V (See Appendix E for the visualization), we can see that both the progressive training strategy and the relational memory unit are individually able to enhance the Informer performance to a certain extent; however, the extent of the improvement is less than when they are combined, thereby indicating that our approach can make effective use of the two components. In addition, each of the components is more effective in the longer sequence settings, thereby suggesting that they are both capable of addressing the difficulties associated with LSTF problems.

Table VI demonstrates the results of our second ablation study, in which we studied the effectiveness of our task-level memory matrix. The first row shows the results of the Informer with the relational memory block that uses our task-level memory matrix, and the second row represents the Informer with the relational memory block that uses the original memory matrix [27]. The results show that our proposed memory matrix approach outperforms the original matrix in both MSE and MAE scores in 11 of 12 prediction tasks, thereby demonstrating that the adaptations we made for the memory matrix can enhance the performance of our relational memory block.

V. CONCLUSION

In this paper, we propose a generalizable memory-driven approach targeting M-LSTF. Our approach is designed to target the specific data characteristics of M-LSTF datasets. We train a global-level memory-driven Transformer-based model in a progressive fashion. We demonstrate that the task-level memory improves the model's ability to comprehend the multivariate sequential patterns from highly similar training samples. In addition, the progressive training schedule can effectively address overfitting issues in LSTF. We validated our methods on five different publicly available datasets with five different prediction lengths ranging from 24 to 720 time steps. The results show that our method works exceptionally well with longer prediction sequences and can achieve up to 30% improvement. Lastly, it is worth noting that to the best of our knowledge, this is the first study that focuses on addressing the particular challenges that arise from M-LSTF.

REFERENCES

- [1] M. Li, W. Cai, R. Liu, Y. Weng, X. Zhao, C. Wang, X. Chen, Z. Liu, C. Pan, M. Li *et al.*, "Ffa-ir: Towards an explainable and reliable medical report generation benchmark," in *Thirty-fifth Conference on Neural Information Processing Systems Datasets and Benchmarks Track (Round 2)*, 2021.
- [2] M. Li, W. Guo, Z. Zhang, W. Yu, and T. Zhang, "Rotated region based fully convolutional network for ship detection," in *IGARSS 2018-2018 IEEE International Geoscience and Remote Sensing Symposium*. IEEE, 2018, pp. 673–676.
- [3] Z. Zhang, W. Guo, M. Li, and W. Yu, "Gis-supervised building extraction with label noise-adaptive fully convolutional neural network," *IEEE Geoscience and Remote Sensing Letters*, vol. 17, no. 12, pp. 2135–2139, 2020.
- [4] M. Li, F. Wang, X. Chang, and X. Liang, "Auxiliary signal-guided knowledge encoder-decoder for medical report generation," *arXiv preprint arXiv:2006.03744*, 2020.
- [5] A. Vaswani, N. Shazeer, N. Parmar, J. Uszkoreit, L. Jones, A. N. Gomez, E. Kaiser, and I. Polosukhin, "Attention is all you need," in *NeurIPS*, 2017.
- [6] S. Hochreiter and J. Schmidhuber, "Long short-term memory," *Neural Computation*, vol. 9, pp. 1735–1780, 1997.
- [7] R. Wen, K. Torkkola, B. Narayanaswamy, and D. Madeka, "A multi-horizon quantile recurrent forecaster," *arXiv:1711.11053*, 2018.
- [8] S. Li, X. Jin, Y. Xuan, X. Zhou, W. Chen, Y.-X. Wang, and X. Yan, "Enhancing the locality and breaking the memory bottleneck of transformer on time series forecasting," in *NeurIPS*, 2019.
- [9] S. Wu, X. Xiao, Q. Ding, P. Zhao, Y. Wei, and J. Huang, "Adversarial sparse transformer for time series forecasting," in *NeurIPS*, 2020.
- [10] H. Zhou, S. Zhang, J. Peng, S. Zhang, J. Li, H. Xiong, and W. Zhang, "Informer: Beyond efficient transformer for long sequence time-series forecasting," in *AAAI*, 2021.
- [11] J. Devlin, M.-W. Chang, K. Lee, and K. Toutanova, "Bert: Pre-training of deep bidirectional transformers for language understanding," in *NAACL*, 2018.
- [12] A. Radford and K. Narasimhan, "Improving language understanding by generative pre-training," 2018.
- [13] L. J. Ba, J. R. Kiros, and G. E. Hinton, "Layer normalization," *CoRR*, vol. abs/1607.06450, 2016. [Online]. Available: <http://arxiv.org/abs/1607.06450>
- [14] L. Li, J. Yan, H. Wang, and Y. Jin, "Anomaly detection of time series with smoothness-inducing sequential variational auto-encoder," *IEEE Trans. Neural Networks Learn. Syst.*, vol. 32, no. 3, pp. 1177–1191, 2021. [Online]. Available: <https://doi.org/10.1109/TNNLS.2020.2980749>
- [15] K. Bandara, C. Bergmeir, and H. Hewamalage, "Lstm-msnet: Leveraging forecasts on sets of related time series with multiple seasonal patterns," *IEEE Trans. Neural Networks Learn. Syst.*, vol. 32, no. 4, pp. 1586–1599, 2021. [Online]. Available: <https://doi.org/10.1109/TNNLS.2020.2985720>
- [16] F. M. Bianchi, S. Scardapane, S. Løkse, and R. Jenssen, "Reservoir computing approaches for representation and classification of multivariate time series," *IEEE Trans. Neural Networks Learn. Syst.*, vol. 32, no. 5, pp. 2169–2179, 2021. [Online]. Available: <https://doi.org/10.1109/TNNLS.2020.3001377>
- [17] F. Rivest and R. Kohar, "A new timing error cost function for binary time series prediction," *IEEE Trans. Neural Networks Learn. Syst.*, vol. 31, no. 1, pp. 174–185, 2020. [Online]. Available: <https://doi.org/10.1109/TNNLS.2019.2900046>
- [18] Q. Tan, M. Ye, A. J. Ma, B. Yang, T. C. Yip, G. L. Wong, and P. C. Yuen, "Explainable uncertainty-aware convolutional recurrent neural network for irregular medical time series," *IEEE Trans. Neural Networks Learn. Syst.*, vol. 32, no. 10, pp. 4665–4679, 2021. [Online]. Available: <https://doi.org/10.1109/TNNLS.2020.3025813>
- [19] H.-Z. Song, D. Rajan, J. J. Thiagarajan, and A. Spanias, "Attend and diagnose: Clinical time series analysis using attention models," in *AAAI*, 2018.
- [20] K. Chen, G. Chen, D. Xu, L. Zhang, Y. Huang, and A. Knoll, "Nast: Non-autoregressive spatial-temporal transformer for time series forecasting," *arXiv:2102.05624*, 2021.
- [21] H. Wu, J. Xu, J. Wang, and M. Long, "Autoformer: Decomposition transformers with auto-correlation for long-term series forecasting," *arXiv:2106.13008*, 2021.
- [22] G. Zerveas, S. Jayaraman, D. Patel, A. Bhamidipaty, and C. Eickhoff, "A transformer-based framework for multivariate time series representation learning," in *SIGKDD*, 2021.
- [23] J. Weston, S. Chopra, and A. Bordes, "Memory networks," in *ICLR*, 2015.
- [24] S. Sukhbaatar, A. Szlam, J. Weston, and R. Fergus, "End-to-end memory networks," in *NeurIPS*, 2015.
- [25] J. Zeng, J. Li, Y. Song, C. Gao, M. R. Lyu, and I. King, "Topic memory networks for short text classification," in *EMNLP*, 2018.
- [26] A. Santoro, R. Faulkner, D. Raposo, J. W. Rae, M. Chrzanowski, T. Weber, D. Wierstra, O. Vinyals, R. Pascanu, and T. Lillicrap, "Relational recurrent neural networks," in *NeurIPS*, 2018.
- [27] Z. Chen, Y. Song, T.-H. Chang, and X. Wan, "Generating radiology reports via memory-driven transformer," in *EMNLP*, 2020.

- [28] M. Li, W. Cai, K. Verspoor, S. Pan, X. Liang, and X. Chang, "Cross-modal clinical graph transformer for ophthalmic report generation," in *Proceedings of the IEEE/CVF Conference on Computer Vision and Pattern Recognition*, 2022, pp. 20 656–20 665.
- [29] M. Jiang, J. Wu, X. Shi, and M. Zhang, "Transformer based memory network for sentiment analysis of web comments," *IEEE Access*, vol. 7, pp. 179 942–179 953, 2019.
- [30] J. Lei, L. Wang, Y. Shen, D. Yu, T. L. Berg, and M. Bansal, "MART: memory-augmented recurrent transformer for coherent video paragraph captioning," in *ACL*, 2020.
- [31] Y. Shi, Y. Wang, C. Wu, C. feng Yeh, J. Chan, F. Zhang, D. Le, and M. Seltzer, "Emformer: Efficient memory transformer based acoustic model for low latency streaming speech recognition," in *ICASSP*, 2021.
- [32] Y. Zhao, C. Ni, C. Leung, S. R. Joty, E. S. Chng, and B. Ma, "Speech transformer with speaker aware persistent memory," in *ISCA*, 2020.
- [33] X. Ma, Y. Wang, M. J. Dousti, P. Koehn, and J. M. Pino, "Streaming simultaneous speech translation with augmented memory transformer," in *ICASSP*, 2021.
- [34] M. Li, P.-Y. Huang, X. Chang, J. Hu, Y. Yang, and A. Hauptmann, "Video pivoting unsupervised multi-modal machine translation," *IEEE Transactions on Pattern Analysis and Machine Intelligence*, 2022.
- [35] R. Du, D. Chang, A. K. Bhunia, J. Xie, Z. Ma, Y. Song, and J. Guo, "Fine-grained visual classification via progressive multi-granularity training of jigsaw patches," in *ECCV*, 2020.
- [36] N. Heidari and A. Iosifidis, "Progressive graph convolutional networks for semi-supervised node classification," *IEEE Access*, vol. 9, pp. 81 957–81 968, 2021.
- [37] B. Pang, G. Peng, Y. Li, and C. Lu, "Pgt: A progressive method for training models on long videos," in *CVPR*, June 2021, pp. 11 379–11 389.
- [38] M. Zhang and Y. He, "Accelerating training of transformer-based language models with progressive layer dropping," in *NeurIPS*, 2020.
- [39] P. Soviany, R. T. Ionescu, P. Rota, and N. Sebe, "Curriculum learning: A survey," *arXiv: 2101.10382*, 2021.
- [40] Y. Bengio, J. Louradour, R. Collobert, and J. Weston, "Curriculum learning," in *ICML*, 2009.
- [41] P. Morerio, J. Cavazza, R. Volpi, R. Vidal, and V. Murino, "Curriculum dropout," in *ICCV*, 2017.
- [42] C. M. Bishop, "Training with noise is equivalent to tikhonov regularization," *Neural Computation*, vol. 7, pp. 108–116, 1995.
- [43] S. Wager, S. I. Wang, and P. Liang, "Dropout training as adaptive regularization," in *NeurIPS*, 2013.
- [44] S. Zhai and Z. Zhang, "Dropout training of matrix factorization and autoencoder for link prediction in sparse graphs," in *SDM*, 2015.
- [45] C. Ma, C. Shen, A. R. Dick, Q. Wu, P. Wang, A. van den Hengel, and I. D. Reid, "Visual question answering with memory-augmented networks," in *CVPR*, 2018.
- [46] C. Ma, L. Ma, Y. Zhang, J. Sun, X. Liu, and M. Coates, "Memory augmented graph neural networks for sequential recommendation," in *AAAI*, 2020.
- [47] Z. Fei, "Memory-augmented image captioning," in *AAAI*, 2021.
- [48] D. Xu, W. Cheng, B. Zong, D. Song, J. Ni, W. Yu, Y. Liu, H. Chen, and X. Zhang, "Tensorized lstm with adaptive shared memory for learning trends in multivariate time series," in *AAAI*, 2020.
- [49] G. Lample, A. Sablayrolles, M. Ranzato, L. Denoyer, and H. Jégou, "Large memory layers with product keys," in *NeurIPS*, 2019.
- [50] K. Fang, A. Toshev, F. Li, and S. Savarese, "Scene memory transformer for embodied agents in long-horizon tasks," in *CVPR*, 2019.
- [51] A. Banino, A. P. Badia, R. Köster, M. J. Chadwick, V. F. Zambaldi, D. Hassabis, C. Barry, M. Botvinick, D. Kumaran, and C. Blundell, "MEMO: A deep network for flexible combination of episodic memories," in *ICLR*, 2020.
- [52] P. Wiryathammabhum, "Spotfast networks with memory augmented lateral transformers for lipreading," in *NeurIPS*, 2020.
- [53] X. Ma, Y. Wang, M. J. Dousti, P. Koehn, and J. Pino, "Streaming simultaneous speech translation with augmented memory transformer," in *ICASSP*, 2021.
- [54] D. Bahdanau, K. Cho, and Y. Bengio, "Neural machine translation by jointly learning to align and translate," in *ICLR*, 2015.
- [55] G. Lai, W.-C. Chang, Y. Yang, and H. Liu, "Modeling long- and short-term temporal patterns with deep neural networks," *ACM SIGIR*, 2018.
- [56] Z. Shen, Y. Zhang, J. Lu, J. Xu, and G. Xiao, "Seriesnet: a generative time series forecasting model," in *IJCNN*, 2018.
- [57] D. H. Wolpert, "The lack of A priori distinctions between learning algorithms," *Neural Comput.*, vol. 8, no. 7, pp. 1341–1390, 1996.